CREEP BEHAVIOR OF FRP-REINFORCED WOOD MEMBERS

By Nikolaos Plevris,[1] Associate Member, ASCE, and Thanasis C. Triantafillou,[2] Member, ASCE

ABSTRACT: In this study, the writers aim to provide a basic understanding of the creep behavior of wood members reinforced with fiber-reinforced plastic (FRP) materials epoxy-bonded to the tension faces. An analytical method is presented first for the deformation of cross sections based on a Burger model combined with a mechanosorptive element for wood, Findley's model for composite materials, and a stress-relaxation procedure to yield the cross-section stresses and strains as a function of time, for both constant and variable temperature and humidity conditions. Parametric studies assessing the effect of the type and area fraction of composite material on the creep response of FRP-reinforced wood members are also presented, for both constant and variable environment. Finally, the analytical model is employed to predict the time-dependent deflections of wood beams reinforced with carbon fiber-reinforced plastic (CFRP) laminates of different thicknesses, and the results of a short experimental program involving FRP-reinforced wood beams under constant environment conditions are also described. The (limited) results are in good agreement with the analytical model.

INTRODUCTION AND BACKGROUND

A considerable amount of research has been conducted in the past to improve the mechanical behavior of structural lumber using reinforcement [e.g., Bulleit (1984)]. Metallic reinforcement has been employed in the form of steel bars, prestressed stranded cables, steel or aluminum plates bonded between laminations, high-strength steel wire embedded in an epoxy matrix through laminations, and stressed steel plates bonded externally using epoxy adhesives [e.g., Bohannan (1962); Sliker (1962); Peterson (1965); Lantos (1970); Krueger (1973); Stern and Kumar (1973); Hoyle (1975); Kobetz and Krueger (1976); Taylor et al. (1983); Dziuba (1985); and Bulleit et al. (1989)]. To improve durability, investigators have also used fiberglass in various forms: as face material of wood-core sandwich panels, as external reinforcement of plywood, and in the form of prestressed strands [e.g., Biblis (1965); Theakston (1965); American Plywood Association (1972); Mitzner (1973); Boehme and Schultz (1974); Saucier and Holman (1975); and Davalos et al. (1992)].

Unless the size of wood elements is a critical design issue, use of fiber-reinforced plastics (FRP) in the compression zone of lumber is not justified. On that basis, Plevris and Triantafillou (1992) provided a comprehensive study of the short-term flexural behavior of wood beams and beam-columns reinforced on the tension face only with epoxy-bonded unidirectional FRP sheets. This work demonstrated that even extremely thin FRP sheets used as external reinforcement of lumber offer many advantages, increasing the strength, stiffness, and ductility characteristics of members considerably. The study was verified experimentally by testing wood beams and beam-columns, which were reinforced with unidirectional carbon fiber-reinforced plastic (CFRP) sheets. Remarkably, CFRP was used for the first time as tension reinforcement of wood in a project involving strengthening of a historic wood bridge near Sins in Switzerland (Meier et al. 1992). This technique of wood reinforcement with composites was further extended by prestressing the FRP sheets before applying them on the wood surface (Triantafillou and Deskovic 1992). Prestressing may be justified when the composite material cost is relatively high, as in the case of CFRP. Analytical models describing the maximum prestress level, so that the FRP-prestressed system does not fail near the two ends of the beam upon releasing the prestressing force, have been developed and verified by Triantafillou and Deskovic (1992).

The work done to date on reinforced wood using FRP sheets as tension reinforcements has focused on short-term response. Here, the writers establish a basic understanding of the creep behavior of FRP-reinforced wood, taking into consideration both constant and variable environmental conditions such as temperature and humidity. An analytical method is described first for the creep deformation of cross sections based on the use of a Burger model combined with a mechanosorptive element for wood (Fridley et al. 1992), Findley's (1960) model for FRP materials, and a stress-relaxation procedure to yield the cross-section stresses and strains as a

[1]Civ. Engrg. Consultant, A. T. Kearney Co., New York, NY.
[2]Lecturer, Dept. of Civ. Engrg., Struct. Div., Univ. of Patras, Patras 26500, Greece.

Note. Discussion open until July 1, 1995. To extend the closing date one month, a written request must be filed with the ASCE Manager of Journals. The manuscript for this paper was submitted for review and possible publication on November 29, 1993. This paper is part of the ***Journal of Structural Engineering***, Vol. 121, No. 2, February, 1995. ©ASCE, ISSN 0733-9445/95/0002-0174–0186/$2.00 + $.25 per page. Paper No. 5979.

function of time. Parametric studies are also presented, to assess the effect of the type and area fraction of composite material on the creep response of FRP-reinforced wood members under both constant and variable temperature and humidity conditions. Finally, the analytical model is employed to predict the time-dependent deflections of wood beams reinforced with CFRP laminates of different thicknesses, and the results of a short experimental program involving FRP-reinforced wood beams under constant environment conditions are also described. The limited test results are in good agreement with the analytical model.

MATERIAL CONSTITUTIVE LAWS

Modeling the time-dependent behavior of FRP-reinforced wood is based on three fundamental considerations: equilibrium of forces and moments, compatibility of strains, and material constitutive relationships. Both wood and FRP are idealized as linear elastic materials; the low stresses resulting in wood from sustained loads are unlikely to cause yielding and plastic deformations in the material.

Wood exhibits strong time-dependent behavior, which is also affected by environmental conditions. Creep strains increase remarkably with humidity and its fluctuation, and with temperature. However, the so-called mechanosorptive processes in wood, that is, the interaction between applied stress and changing moisture content exhibited in the creep behavior, are currently not fully understood [e.g., Tang (1980); van der Put (1989a and 1989b); and Toratti (1991)]. Recently, Fridley et al. (1992) developed a comprehensive model to describe the observed primary and secondary creep behavior of wood under constant and step-constant load histories and a variety of constant and cyclic hygrothermal conditions. The model is based on a Burger element modified to account for hygrothermal effects (see Fig. 1), and is given in differential form, as follows:

$$\dot{\varepsilon} = \dot{\varepsilon}_e + \dot{\varepsilon}_k + \dot{\varepsilon}_v + \dot{\varepsilon}_{ms} \tag{1}$$

in which $\dot{\varepsilon}$ = total time rate of strain; $\dot{\varepsilon}_e$ = elastic time rate of strain; $\dot{\varepsilon}_k$ = viscoelastic (Kelvin) time rate of strain; $\dot{\varepsilon}_v$ = time rate of viscoplastic strain; and $\dot{\varepsilon}_{ms}$ = time rate of mechanosorptive strain. The mathematical expressions for the four component rates of strain are

$$\dot{\varepsilon}_e = \frac{\dot{\sigma}}{K_e}; \quad \dot{\varepsilon}_k = \frac{\sigma}{\mu_k} - \varepsilon_k \frac{K_k}{\mu_k}; \quad \dot{\varepsilon}_v = \frac{\sigma}{\mu_v}; \quad \dot{\varepsilon}_{ms} = \frac{\sigma}{\mu_{ms}} = \frac{\sigma|\dot{\omega}|}{\mu'_{ms}} \tag{2, 3, 4, 5}$$

in which σ = applied stress; $\dot{\sigma}$ = time rate of applied stress; K_e = Hookean spring constant associated with elastic deformation; K_k and μ_k = Hookean spring constant and viscosity of the Newtonian dashpot, respectively, of the Kelvin element; ε_k = Kelvin strain (delayed elastic strain); μ_v = viscosity of the Newtonian dashpot associated with unrecoverable strain; μ_{ms} = viscosity of the mechanosorptive element; μ'_{ms} = a constant with units of stress; and $\dot{\omega}$ = rate of change in the relative moisture content factor with units of inverse time.

Defining the relative moisture content factor ω and the relative temperature factor θ as follows:

$$\omega = \frac{M - M_0}{M_0}; \quad \text{and} \quad \theta = \frac{T - T_0}{T_0} \tag{6, 7}$$

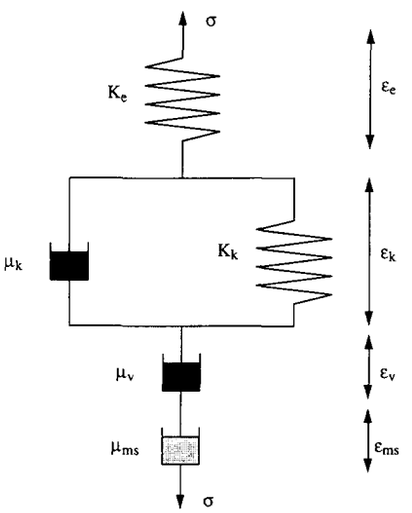

FIG. 1. Five-Element Creep Model for Wood

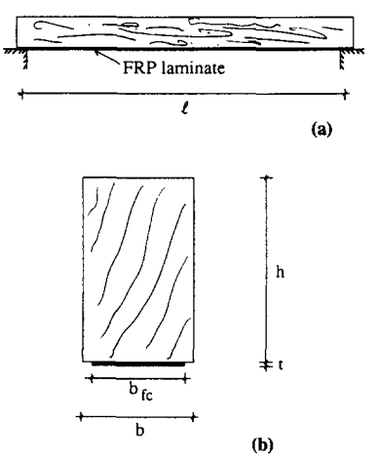

FIG. 2. (a) Wood Beam Reinforced with FRP Laminate; (b) Its Cross Section

in which M = actual moisture content; M_0 = a reference moisture content; T = actual temperature; and T_0 = a reference temperature, Fridley et al. (1992) assumed the following functions for the model parameters:

$$K_e = K_{e0}(1 + D_1\omega + D_2\omega^2 + D_3\theta + D_4\theta^2); \quad K_k = K_{k0}(1 + D_5\omega + D_6\omega^2 + D_7\theta + D_8\theta^2) \tag{8, 9}$$

$$\mu_k = \mu_{k0}(1 + D_9\omega + D_{10}\omega^2 + D_{11}\theta + D_{12}\theta^2); \quad \mu_v = \mu_{v0}(1 + D_{13}\omega + D_{14}\omega^2 + D_{15}\theta + D_{16}\theta^2) \tag{10, 11}$$

Here K_{e0}, K_{k0}, μ_{k0}, and μ_{v0} = model parameters in the reference condition $\omega = \theta = 0$, and D_1–D_{16} = model constants. Note that K_{e0}, K_{k0}, μ_{k0}, and μ_{v0} are functions of moisture and temperature, which are in turn functions of time.

From (2)–(5), the strain ε at time t caused by a constant stress σ is as follows:

$$\varepsilon(t) = \varepsilon_e(t) + \varepsilon_k(t) + \varepsilon_v(t) + \varepsilon_{ms}(t) \tag{12}$$

in which

$$\varepsilon_e(t) = \frac{\sigma}{K_e(t)}; \quad \varepsilon_k(t) = \varepsilon_k(t - dt) + \dot{\varepsilon}_k(t - dt)\, dt \tag{13, 14}$$

$$\varepsilon_v(t) = \varepsilon_v(t - dt) + \frac{\sigma}{\mu_v(t)}\, dt; \quad \varepsilon_{ms}(t) = \varepsilon_{ms}(t - dt) + \frac{\sigma|\dot{\omega}|}{\mu'_{ms}}\, dt \tag{15, 16}$$

Note that the boundary conditions used to perform the numerical integration include $\varepsilon_k(0) = 0$ and $\dot{\varepsilon}_k(0) = \sigma/\mu_k(0)$. Finally, the constitutive law describing the creep behavior of wood is written as follows:

$$\varepsilon(t) = \frac{\sigma}{E_{\text{eff}}(t)} \tag{17}$$

in which $E_{\text{eff}}(t)$ = effective modulus of wood, defined as follows:

$$E_{\text{eff}}(t) = E_w \frac{\varepsilon(0)}{\varepsilon(t)} \tag{18}$$

Here, E_w = initial elastic modulus of wood. For constant temperature and humidity conditions, E_{eff} is obtained as follows:

$$\frac{1}{E_{\text{eff}}} = \frac{1}{K_e} + \frac{1}{K_k}\left[1 - \exp\left(\frac{K_k t}{\mu_k}\right)\right] + \frac{t}{\mu_v} \tag{19}$$

A reliable and simple creep model for composite materials is based on a power law expression proposed by Findley (1960). The general form of this expression, which applies well to linear viscoelastic material characterization at constant temperature, is as follows:

$$\varepsilon = \varepsilon_0 + m\left(\frac{t}{t_0}\right)^n \tag{20}$$

in which ε = time-dependent strain; ε_0 = initial strain; m = function of stress; and n and t_0 = material constants (t_0 may be taken as unity). Note that the effect of temperature on the creep of composites is primarily associated with the response of the matrix. Hence, for unidirectional composites with a high-fiber-volume fraction (in the order of 60%), the effect of temperature variations on creep behavior can be neglected. From the creep model of (20), a viscoelastic modulus E_v can be obtained as follows:

$$E_v = \frac{E_0 \dfrac{\sigma}{m}}{\dfrac{\sigma}{m} + E_0\left(\dfrac{t}{t_0}\right)^n} \tag{21}$$

in which E_0 = initial elastic modulus of the FRP material. Eq. (21) is the constitutive law describing the creep behavior of FRP laminates in tension.

ANALYSIS OF CROSS SECTIONS

In the following, it is assumed that plane sections remain plane, the bond at the wood-FRP interface is perfect, and time effects in the adhesive are negligible. These assumptions are justified because: (1) For a thin layer of epoxy adhesive, the ratio of bond line to bond thickness is very high, so that even if the adhesive creeps in shear (especially near the ends of the FRP, where

the interface shear stresses are higher) the resulting normal strains in the laminate are negligible; (2) the high stiffness of the laminate will prevent the part of adhesive creep caused by normal stresses; and (3) shrinkage and swelling of wood (under variable environment) is much higher in the transverse direction (perpendicular to the member axis), so that longitudinal microcracks may develop in the adhesive (although the laminate's very low modulus of elasticity in the transverse direction is quite favorable for inhibiting such cracking). These microcracks are not as critical for members in bending, and will have no major effect on the FRP laminate, which is primarily reinforced with fibers in the longitudinal direction.

Short-Term Analysis

A typical wood beam reinforced with an FRP laminate is illustrated in Fig. 2. The wood section has height h and width b, and the laminate has thickness t and width b_{fc}. Fig. 3 shows the strain and stress distribution in a cross section under bending moment M and axial force N, both referred to the top wood fiber. The strain distribution at $t = 0$ is defined by the initial strain ε_{0i} of the top wood fiber and the initial curvature κ_i. At a distance y from the top fiber, the strain is given as follows:

$$\varepsilon_i = \varepsilon_{0i} - y\kappa_i \tag{22}$$

Equilibrium of horizontal forces and moments gives the following expression for N and M:

$$N = \int_0^h E_w(\varepsilon_{0i} - y\kappa_i)b\,dy + E_0(\varepsilon_{0i} - h\kappa_i)b_{fc}t; \quad M = \int_0^h E_w(\varepsilon_{0i} - y\kappa_i)yb\,dy - E_0(\varepsilon_{0i} - h\kappa_i)hb_{fc}t \tag{23, 24}$$

The assumption in (22) and (23) is that the thickness t of the FRP laminate is very small compared with the height of the cross section.

Subsequently, following the method of Gilbert (1988) for the analysis of cross sections, and rearranging (23) and (24) we obtain the following:

$$\varepsilon_{0i} = \frac{BM + IN}{AI - B^2}; \quad \kappa_i = \frac{AM + BN}{AI - B^2} \tag{25, 26}$$

where

$$A = E_w bh + E_0 b_{fc} t; \quad B = \frac{1}{2} E_w bh^2 + E_0 b_{fc} th; \quad I = \frac{1}{3} E_w bh^3 + E_0 b_{fc} th^2 \tag{27, 28, 29}$$

Creep Analysis

The change in strain and curvature that occurs in the cross section over time is illustrated in Fig. 4. For the creep analysis of the cross section, a relaxation method first proposed by Bresler and Selna (1964) was adopted. At any time interval the total strains are considered initially unchanged. Hence, while the creep strains change, the elastic strains change by an equal and opposite amount, as do the stresses, resulting in a change of the internal force and moment. To restore equilibrium, an axial force ΔN and a bending moment ΔM must be applied to the section, which responds according to the effective material moduli. The change in strain due to creep is prevented by the restraining action $-\Delta N$ and $-\Delta M$. Applying ΔN and ΔM to the cross section, the restraining actions are removed and equilibrium is restored. This approach has been followed in a number of studies of the creep and shrinkage analysis of concrete or composite steel-concrete structures and for the analysis of cross section in two or three-dimensional problems (Ghali and Favre 1986; Gilbert 1988; Bradford and Gilbert 1990; Adrian and Triantafillou 1992). Recently, the same approach was followed by Plevris and Triantafillou (1994) to study the time-dependent behavior of concrete beams strengthened with FRP laminates. ΔM and ΔN produce increments of ε_{0i} and κ_i, which are calculated as follows:

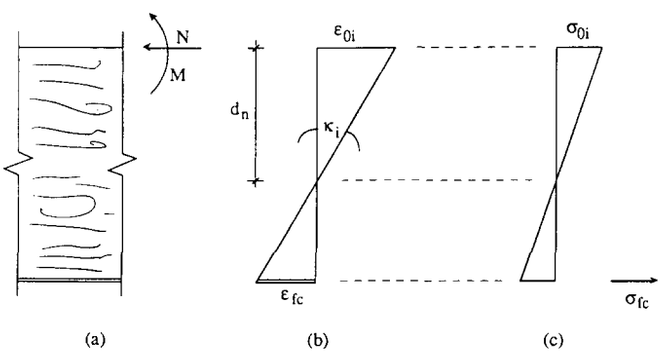

FIG. 3. (a) Elevation; (b) Initial Strain Distribution; and (c) Initial Stress Distribution

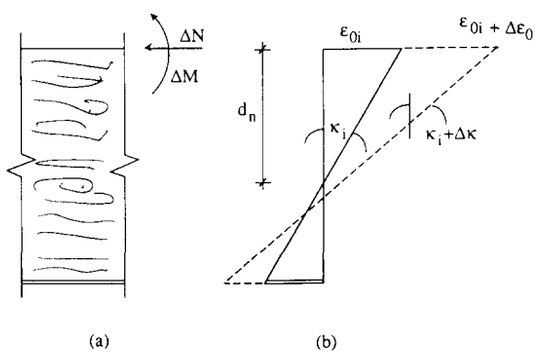

FIG. 4. (a) Elevation; (b) Time-Dependent Strain Distribution

$$\Delta\varepsilon_0 = \frac{\bar{B}\Delta M + \bar{I}\Delta N}{\bar{A}\bar{I} - \bar{B}^2}; \quad \Delta\kappa = \frac{\bar{A}\Delta M + \bar{B}\Delta N}{\bar{A}\bar{I} - \bar{B}^2} \tag{30, 31}$$

in which the time-adjusted quantities $\bar{A}$, $\bar{B}$, and $\bar{I}$ are given by (27)–(29) using E_{eff} and E_v instead of E_w and E_0, respectively. From (23) and (24), the creep restraining actions are obtained as follows:

$$-\Delta N = -E_{eff}\beta\left(bh\varepsilon_{0i} - \frac{1}{2}bh^2\kappa_i\right) - E_v\alpha(\varepsilon_{0i} - h\kappa_i)b_{fc}t \tag{32}$$

$$-\Delta M = -E_{eff}\beta\left(-\frac{1}{2}bh^2\varepsilon_{0i} + \frac{1}{3}bh^3\kappa_i\right) + E_v\alpha(\varepsilon_{0i} - h\kappa_i)b_{fc}th \tag{33}$$

in which α and β = FRP and wood creep coefficients, respectively, defined as follows:

$$\alpha = \frac{E_0}{E_v} - 1; \quad \beta = \frac{E_w}{E_{eff}} - 1 \tag{34, 35}$$

The final stresses in the wood at a distance y below the top fiber (σ_w) and in the FRP laminate (σ_{fc}) are calculated by adding to the initial values the change of stress due to: (1) Relaxation while the strain is frozen; and (2) the application of ΔN and ΔM. The result is as follows:

$$\sigma_w = E_w(\varepsilon_{0i} - y\kappa_i) - E_w\beta(\varepsilon_{0i} - y\kappa_i) + E_{eff}(\Delta\varepsilon_0 - y\Delta\kappa) \tag{36}$$

$$\sigma_{fc} = E_0(\varepsilon_{0i} - h\kappa_i) - E_v\alpha(\varepsilon_{0i} - h\kappa_i) + E_v(\Delta\varepsilon_0 - h\Delta\kappa) \tag{37}$$

It is true that the creep analysis presented here could be simplified; the traditional transformed section approach would be easier to apply to simple cross sections such as the one analyzed previously. However, the procedure presented here is easily programmed and ideal for the analysis of irregularly shaped sections or cross sections containing a number of FRP laminates at different levels.

PARAMETRIC STUDIES

The formulation described in the previous sections was implemented in a computer program that was used to carry out a series of parametric studies. The studies aimed at investigating the time effect of the FRP type and area fraction on the curvature, κ, the wood top and bottom fiber stresses, σ_{wt} and σ_{wb}, respectively, and the stress in the fiber composite, σ_{fc}, at both constant and variable environmental conditions. Three types of composites were considered, namely, CFRP, AFRP (aramid fiber-reinforced plastic), and GFRP (glass fiber-reinforced plastic), at four different area fractions. The laminate area fractions varied not only for a given material (four different ρ_{fc} were employed for each FRP type) but also for the various types of materials, to ensure that the same four axial rigidities ($E_0b_{fc}t$) were assigned to all three types of laminates. Finally, the initial elastic modulus of wood was taken as E_w = 12.7 GPa.

Eq. (21) was calibrated from data on the creep behavior of carbon, aramid, and glass fibers, and typical epoxy matrices, at a fiber volume fraction of about 60% (Sturgeon 1978; Preis and Bell 1986; Phillips 1989). The parameters obtained from application of Findley's model to the three composites are summarized in Table 1; the resulting viscoelastic moduli are given in Fig. 5. As expected, AFRP is characterized by higher creep strains compared with the other composites (see decrease of E_v with time in Fig. 5), which is attributed to the relatively high creep response of aramid fibers, especially during a short period after loading.

Constant Environment

For constant temperature and moisture conditions, the values adopted for the wood creep model are summarized in Table 2. These values represent the mean over many experimental results on Select Structural and No. 2 Douglas fir lumber, as described by Fridley et al. (1992). The resulting effective modulus of wood as a function of time is shown in Fig. 6.

The time effect of FRP type and area fraction on the normalized curvature κ of a reinforced wood cross section is illustrated in Fig. 7. The initial curvature decreases considerably by increasing the FRP area fraction. Yet, the development of creep curvature with time is substantial

TABLE 1. Composite Material Properties Used in Parametric Study

Material (1)	E_0 (GPA) (2)	σ_0/m (GPA) (3)	n (4)	t_0 (days) (5)
CFRP	182	62,670	0.123	0.0417
AFRP	79	620	0.129	0.0417
GFRP	44	1,780	0.061	0.0417

TABLE 2. Reference Environment Wood Properties

Variable (1)	Value (2)
K_{r0} (GPa)	12.7
K_{k0} (GPa)	26.7
μ_{k0} (GPa-day)	314
μ_{v0} (GPa-day)	358×10^4

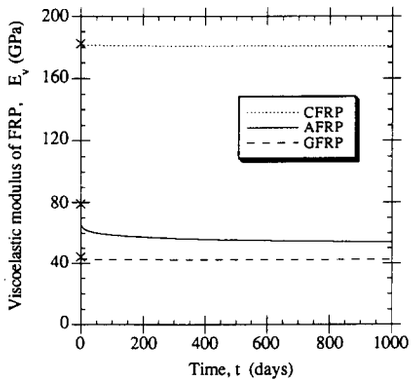

FIG. 5. Viscoelastic FRP Moduli Assumed in Parametric Studies

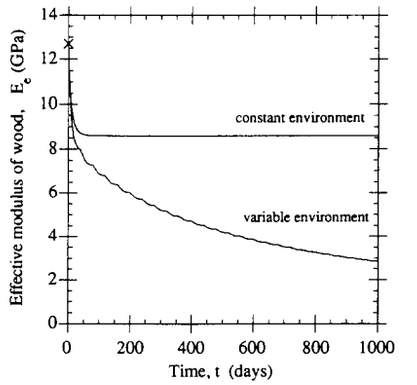

FIG. 6. Effective Modulus of Wood Assumed in Parametric Studies

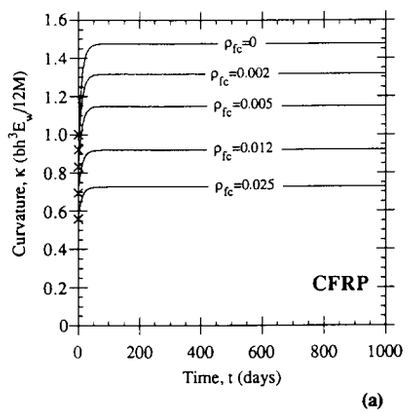

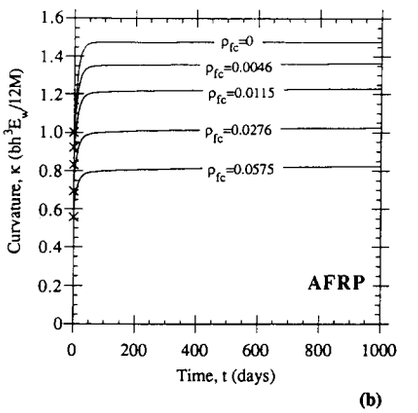

FIG. 7. Effect of FRP Type and Area Fraction on Curvature; (a) CFRP; (b) AFRP

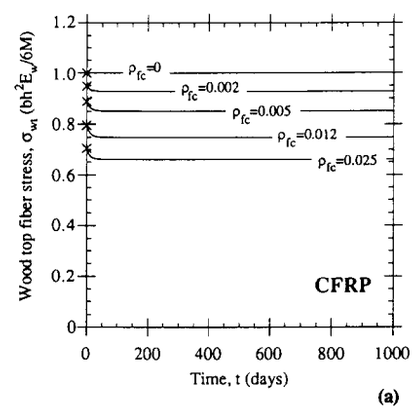

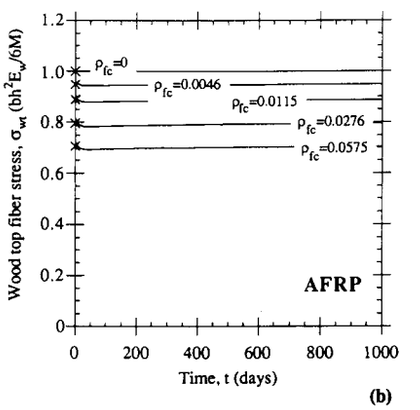

FIG. 8. Effect of FRP Type and Area Fraction on Wood-Top Fiber Stress: (a) CFRP; (b) AFRP

in the first 50 days of loading and much slower afterwards, indicating that creep of wood is the dominant deformation mechanism (note the reduction of E_{eff} in the first 50 days shown in Fig. 6). Therefore, it appears that the type of FRP employed to reinforce wood is of little importance in controlling deflections; far more important is the area of reinforcement. In Figs. 8–10, the plots corresponding to GFRP are omitted, due to the nearly identical creep response of GFRP to that of CFRP.

Next, Fig. 8 shows that the initial normalized wood top fiber stress σ_{wt} decreases with increasing ρ_{fc}. Furthermore, only small reductions of the stress are expected over time when CFRP (or GFRP) laminates are used, while when AFRP is used it may even result in small increases of the stress during the first few hours or days, due to its high creep characteristics displayed in the early stages of loading (Fig. 5).

The time effect of the FRP type and area fraction on the normalized wood-bottom fiber stress σ_{wb} is illustrated in Fig. 9. Here, the laminates reduce the tensile stresses in wood remarkably

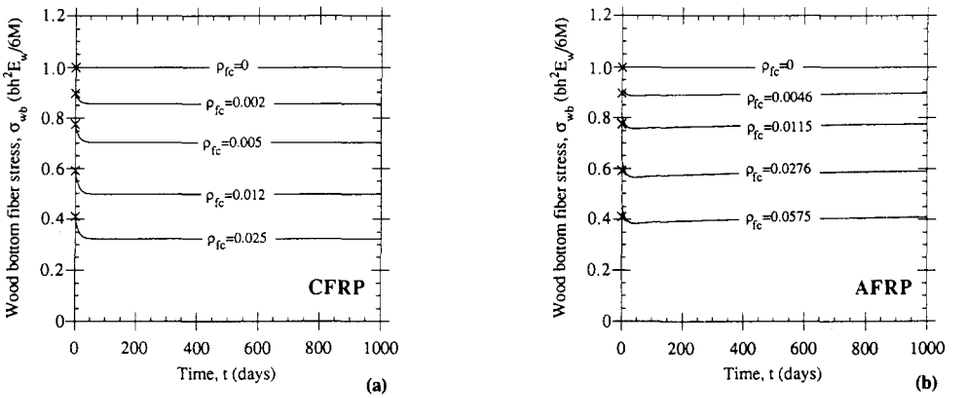

FIG. 9. Effect of FRP Type and Area Fraction on Wood-Bottom Fiber Stress: (a) CFRP; (b) AFRP

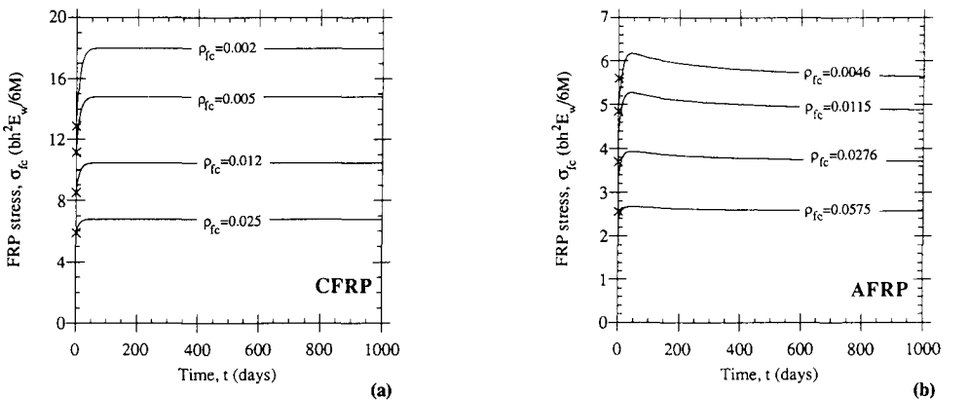

FIG. 10. Effect of FRP Type and Area Fraction on Laminate Stress: (a) CFRP; (b) AFRP

with increasing ρ_{fc}. In addition, the long-term stress reduction over time is considerable with CFRP (or GFRP) and rather negligible with AFRP; due to its creep characteristics, AFRP causes a small initial increase of σ_{wb} in the first few hours or days of loading, which balances the stress decrease recorded afterwards.

The change of normalized FRP stress σ_{fc} over time is given in Fig. 10. For the case of CFRP (or GFRP), increasing ρ_{fc} decreases not only the initial but also the long-term stress. On the other hand, AFRP gives an interesting response: σ_{fc} drops a little in the first few hours or days (due to the high creep of the laminate), increases as long as the wood creeps considerably, and then decreases slightly after about 50 days of loading, when the rate of creep of wood becomes lower than that of AFRP.

In summary, the response of the section reinforced with either CFRP or GFRP is quite similar, while the use of AFRP results in curvatures and stresses that are slightly higher than those obtained with the other composites, except for the long-term stress in the laminate.

Variable Environment

The creep behavior of FRP-reinforced wood is considered here for an environmental history based on a reference temperature of 22.8°C, a 50% relative humidity (RH), and a 40-day period cycling in the range 6.8–22.8°C and 40–60% RH for a total of 1,000 days. The relative temperature factor θ and the environment moisture factor ω_e are 0 and 0.2, respectively, for $0 < t < 20$ days, $40 < t < 60$ days and so forth, while the associated values of θ and ω_e for $20 < t < 40$ days, $60 < t < 80$ days and so forth are -0.4 and -0.2. Since the objective here is basically to make only qualitative arguments regarding the effect of FRP area fraction on the creep behavior of wood members under thermal and humidity cycling, the environmental fluctuations assumed are entirely hypothetical.

Next, an assumption is made that the temperature in a wood member is qual to that of the environment. The same argument does not hold for the moisture content, which changes gradually over time inside the member. Following Fridley et al. (1992) the average moisture-content factor of a wood specimen at a time t_ω following an abrupt change in the surrounding environment is assumed as follows:

$$\omega(t_\omega) = \omega_f + (\omega_i - \omega_f)\exp(-B_\omega t_\omega) \tag{38}$$

in which ω_f and ω_i = final and initial environment moisture factors, respectively; and B_ω = a constant dependent on the member size, associated with the time required to achieve moisture equilibrium. Applying (38) to the environmental moisture history just described (assuming $B_\omega = 2.1 \times 10^{-5}\ \text{min}^{-1}$), the relative moisture content factor ω was obtained as shown in Fig.

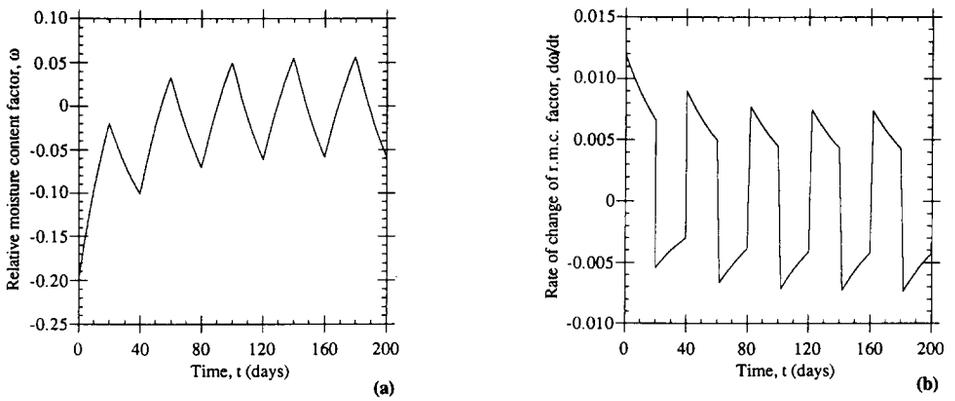

FIG. 11. Environmental History Assumed in Parametric Study: (a) Wood-Relative-Moisture-Content Factor; and (b) Rate of Change of Wood-Relative-Moisture-Content Factor

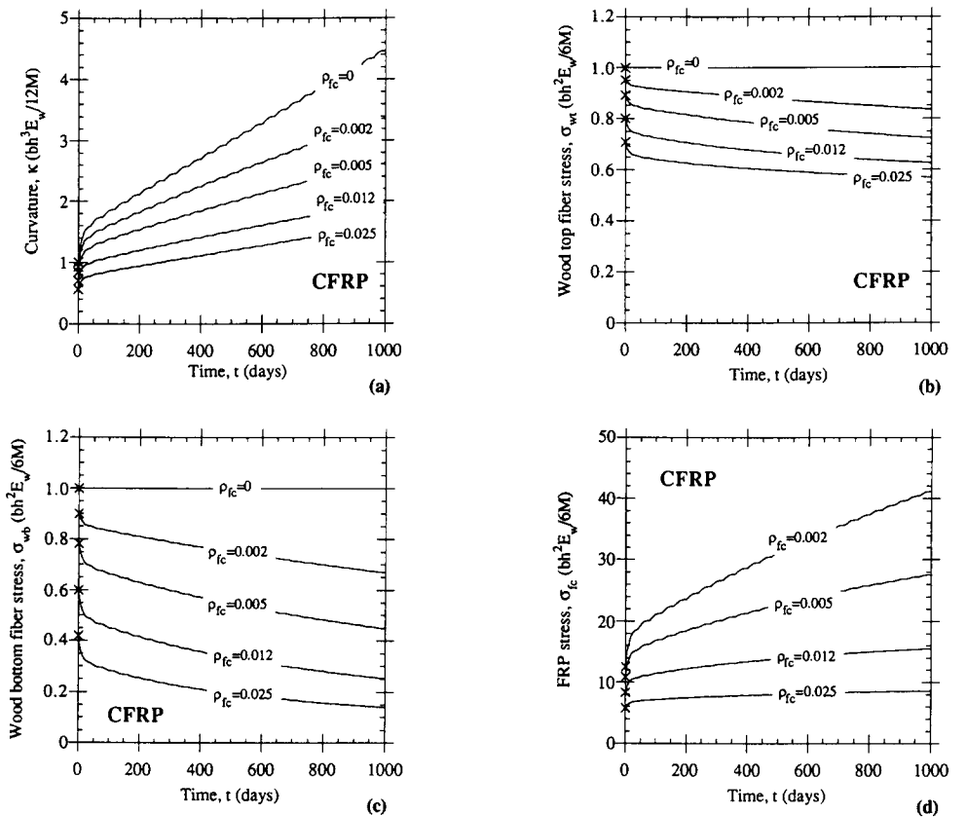

FIG. 12. Comparison of Response Parameters for Different CFRP Area Fractions and Variable Environment: (a) Curvature; (b) Wood Top Fiber Stress; (c) Wood Bottom Fiber Stress; and (d) Laminate Stress

TABLE 3. CFRP Area Fraction of Beams Tested

Beam # (1)	t (mm) (2)	b_{fc} (mm) (3)	ρ_{fc} (4)
1	—	—	—
2	1.016	45	0.0118
3	1.372	45	0.0165

TABLE 4. Wood Properties as Calibrated from Experiment

Variable (1)	Value (2)
K_c (GPa)	9.62
K_k (GPa)	84.4
μ_k (GPa-day)	194
$\mu_{k'}$ (GPa-day)	1.14×10^4

11(a); the associated rate of change of ω is given in Fig. 11(b). Finally, in order to apply the creep models presented earlier for FRP-reinforced wood members, the following functions for the model parameters were assumed:

$$K_c = K_{c0}(1.002 - 0.173\omega + 0.008\omega^2 - 0.012\theta) \quad (39)$$

$$K_k = K_{k0}(0.994 - 0.630\omega + 0.173\omega^2 - 0.032\theta) \quad (40)$$

$$\mu_k = \mu_{k0}(0.990 - 0.653\omega + 0.142\omega^2 - 0.041\theta) \quad (41)$$

$$\mu_c = \mu_{c0}(0.992 - 0.575\omega + 0.146\omega^2 - 0.005\theta) \quad (42)$$

These parameters were proposed by Fridley et al. (1992) as a result of statistical manipulation of a large number of test data for Select Structural and No. 2 Douglas fir lumber; based on the same study, the mechanosorptive constant was taken as $\mu'_{ms} = 26.04$ GPa. The resulting effective modulus of wood for the environmental history described above is plotted in Fig. 6.

Now, the time effect of the composite laminate area fraction on the curvature, the wood top and bottom fiber stresses, and the laminate stress are evaluated based on the results illustrated in Fig. 12, for the case of wood reinforced with CFRP. The normalized creep curvatures [Fig. 12(a)] are dominated by two factors: (1) Hygrothermal cycling on K_c, K_k, μ_k and μ_c; and (2) action of the mechanosorptive element. Apparently, increasing ρ_{fc} makes the effect of these two factors much less pronounced, resulting in considerable decreases of the creep deformations. In addition, Figs. 12(b and c) show that increasing the composite reinforcement area fraction produces remarkable decreases in the wood stresses. However, the stress decrease in wood comes at the expense of substantial increase of the stress in the reinforcement [Fig. 12(d)], an essential factor in the selection of the laminate. For instance, consider a CFRP area fraction as low as 1.2%. This reinforcement decreases the ratio of the 1,000-day creep to initial curvature from 3.5 (when no reinforcement is used) to 1.8, a reduction of about 50%. At the same time, the same amount of reinforcement reduces the wood top and bottom fiber stresses by about 25% and 60%, respectively. But, it is important to note that the laminate stress increases by about 200% (which, given the extremely high strength of advanced composites, is rather unlikely to be a major concern).

EXPERIMENTAL METHOD

To verify the part of the analysis for the effect of FRP-reinforcement on the creep response of wood beams under constant environment conditions, a short experimental program was carried out on three fir lumber beams, obtained from the same piece of wood. Two of the beams were reinforced with epoxy-bonded CFRP laminates of different thickness (after both the wood and CFRP surfaces were roughened and cleaned), and a third was used as a control specimen. The beams were loaded in three-point bending at a span of 1,486 mm under a sustained load, under controlled constant temperature (about 20°C) and humidity (about 50% RH) conditions.

Each beam was 1,664 mm long and had a cross section 45 mm wide and 86 mm deep. The unidirectional CFRP sheets were made of high-modulus carbon fibers at a volume fraction of about 65%, bonded together with an epoxy matrix. According to the CFRP supplier, the laminates had an elastic modulus of 186 GPa and a tensile strength of 1,450 MPa. The CFRP area fraction for each of the beams tested is given in Table 3. It should be emphasized that even though the beams tested were not quite representative of real size members, the relative effect of various CFRP area fractions on creep behavior could still be demonstrated.

The load was applied through air diaphragm cylinders. Two of the beams were loaded against each other, and the third was loaded against an aluminum beam. One member of each pair was attached to the base of the air cylinder and the other to the cylinder piston, so that the only load carried by the loading frame was that of the weight of the two beams. The resulting actual load for beams 1, 2, and 3 was 2.63 kN, 2.83 kN, and 2.76 kN, respectively; these values also account for the self-weight of the beams (which, for the inverted beam, acts opposite to the applied load). The pressurized air was provided by a main electric compressor. The air filled a buffer tank first, and then through precision regulators went to the cylinders. To enhance the reliability of the system, a back-up device was also installed. First, a pressure sensor recorded the input pressure; if the pressure dropped below a certain value (higher than that required for the cylinders), a valve would provide pressurized nitrogen from a high pressure container to the buffer tank, after passing through a course regulator. At the same time another value would close, to prevent leakage of nitrogen to the main air-pressure system. Upon recovery of the air pressure, the two values would return automatically to their initial positions. A schematic illustration of the experimental setup is given in Fig. 13 (the same setup was also used by the writers in a parallel research program to investigate the long-term behavior of concrete beams strengthened with CFRP laminates).

The pressure of the nitrogen tank had to be checked periodically, so that it could be replaced if necessary. It was found that three months after application of the load the pressure drop was

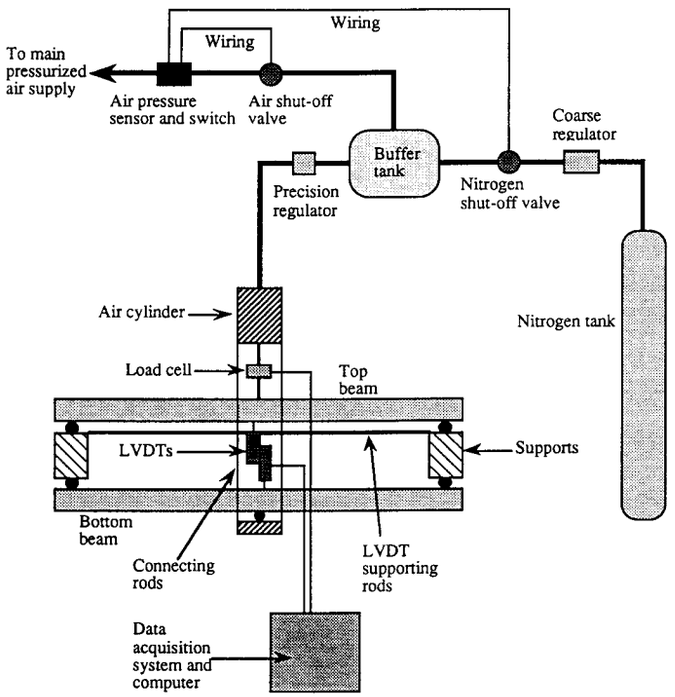

FIG. 13. Schematic Illustration of Experimental Setup

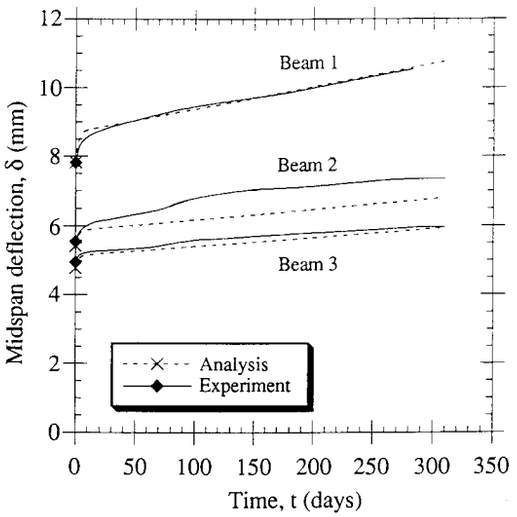

FIG. 14. Midspan Deflection versus Time: Comparison of Analysis with Experiments

less than 50%. Furthermore, load measurements over the same period of time indicated no significant load fluctuations.

The midspan deflections were measured with linear voltage differential transducers, and the loads were measured with load cells attached to the piston heads. The analog signals provided by the instruments were digitized by a data acquisition system and then recorded by a personal computer at predefined time intervals, ranging from 10 sec at the beginning of the experiment, to 4 hr after 5 months.

RESULTS

The recorded midspan deflections over the first 10 months of loading for the different beam designs are given by the solid curves of Fig. 14. As expected, increasing the CFRP area fraction decreases both the immediate and the creep deflections. The response characteristics of the beam without CFRP reinforcement (beam 1) were used to calibrate the analytical model. First, the initial elastic modulus of wood was calculated based on the immediate deflection of the beam, and it was found to be $E_w\ (=K_e) = 9.62$ GPa. Then, the remaining parameters of the wood creep model applied for constant environment were obtained based on least squares fit, and are summarized in Table 4. Unidirectional CFRP is creep-free, so that $E_c = E_0$ was assumed for the laminate.

The results of this calibration were then used for the analytical prediction of the response of the other two beams, as shown in Fig. 14 (beams 2 and 3, dashed lines). It is seen that the immediate deflection is predicted with high accuracy. Furthermore, the agreement between experiment and analysis is excellent for beam 3 (the maximum discrepancy in total deflections is less than 5%), and reasonable for beam 2: the maximum error for beam 2 is less than 10% for the total deflection and approaches 40% for the creep deflection. But given the high variability characterizing wood properties, the last figure should not be surprising at all. Overall, despite its simplifying assumptions, the procedure presented in this study gave a reasonably good prediction of the effect of FRP reinforcement on the creep response of reinforced wood members under constant environment conditions.

CONCLUSIONS

In the present study, the writers developed a general analytical model for predicting the creep response of wood members reinforced with externally epoxy-bonded unidirectional laminates, under constant and variable temperature and humidity conditions. Parametric studies based on the analysis of cross sections led to the following conclusions: The creep behavior of FRP-reinforced wood is primarily dominated by the creep of wood. For constant environment, increasing the area fraction of composite plays a significant role in controlling deformations,

but the type of composite influences the behavior very little, if at all. Moreover, with CFRP and GFRP there is a slight transfer of stresses from the wood in the tension zone to the laminate. For variable temperature and humidity conditions, the role of reinforcement in controlling deflections becomes far more pronounced. Yet, the transfer of stresses from wood to FRP is considerable, indicating that selection of the laminate thickness should be based on a high safety factor. The implication is that GFRP, a material with low strength under sustained tension (and questionable durability), should be used with caution. For other composites, it is believed that the stress transfer will cause no problem at all, due to the high strength characterizing these materials.

The limited experimental results obtained in this study were in agreement with the part of the analysis associated with the effect of different reinforcement areas on the long-term deflections of FRP-reinforced beams under constant environmental conditions. Furthermore, it was demonstrated that CFRP is an excellent material to be used as flexural reinforcement of wood: a CFRP area fraction of just a little over 1% reduced the total member deflections by about 40%, and the creep deflections by more than 50%. It is clear that the experimental database should be expanded; future studies should provide creep and durability test data for FRP-reinforced wood under cyclic humidity and temperature conditions.

ACKNOWLEDGMENTS

This project was partially supported by a grant from the U.S. Army Research Office through the program for Advanced Construction Technology at M.I.T., and by the National Science Foundation (grant No. MSS-9015542). The authors wish to thank Dr. J. Germaine for his invaluable assistance in designing the experimental program.

APPENDIX I. REFERENCES

Adrian, C. A., and Triantafillou, T. C. (1992). "Creep and shrinkage analysis of composite systems under axial load and biaxial bending." *Mat. and Struct., RILEM*, Paris, France, Vol. 25, 543–551.

American Plywood Association (1972). "Basic panel properties of plywood overlaid with fiberglass-reinforced plastic." *Am. Plywood Assoc. Res. Rep. No. 119, Part 1*, Madison, Wisc.

Bradford, M. A., and Gilbert, R. I. (1990). "Time-dependent analysis and design of composite columns." *J. Struct. Engrg.*, ASCE, 116(12), 3338–3357.

Bresler, B., and Selna, L. (1964). "Analysis of time dependent behavior of reinforced concrete structures." *Symp. on Creep of Concrete, ACI Spec. Publ. SP-9(5)*, American Concrete Institute, Detroit, Mich., 115–128.

Boehme, C., and Schultz, U. (1974). "Load bearing behavior of a GFRP sandwich." *Holz Roh-Werkst*, 32(7), 250–256 (in German).

Bohannan, B. (1962). "Prestressed wood members." *Forest Products J.*, 12(12), 596–602.

Biblis, E. J. (1965). "Analysis of wood-fiberglass composite beams within and beyond the elastic region." *Forest Products J.*, 15(2), 81–88.

Bulleit, W. M. (1984). "Reinforcement of wood materials: a review." *Wood and Fiber Sci.*, 16(3), 391–397.

Bulleit, W. M., Sandberg, L. B., and Woods, G. J. (1989). "Steel-reinforced glued laminated timber." *J. Struct. Engrg.*, ASCE, 115(2), 433–444.

Davalos, J. F., Salim, H. A., and Munipalle, U. (1992). "Glulam-GFRP composite beams for stress-laminated T-system bridges." *Proc., 1st Int. Conf. on Advanced Composite Mat. in Bridges and Struct.*, Can. Soc. for Civ. Engrs., Sherbrooke, Canada, 455–466.

Dziuba, T. (1985). "The ultimate strength of wooden beams with tension reinforcement." *Holzforschung und Holzverwertung*, 37(6), 115–119 (in German).

Findley, W. N. (1960). "Mechanism and mechanics of creep of plastics." *SPE J.*, (Jan.), 57–65.

Fridley, K. J., Tang, R. C., and Soltis, L. A. (1992). "Creep behavior model for structural lumber." *J. Struct. Engrg.*, ASCE, 118(8), 2261–2277.

Ghali, A., and Favre, R. (1986). *Concrete structures: stresses and deformations*. Chapman & Hall, Ltd., London, England.

Gilbert, R. I. (1988). *Time effects in concrete structures*. Elsevier Science Publishers, Amsterdam.

Hoyle, R. J. (1975). "Steel-reinforced wood beam design." *Forest Products J.*, 25(4), 17–23.

Kobetz, R. W., and Krueger, G. P. (1976). "Ultimate strength design of reinforced timber: biaxial stress failure criteria." *Wood Sci.*, 8(4), 252–262.

Krueger, G. P. (1973). "Ultimate strength design of reinforced timber: State of the art." *Wood Sci.*, 6(2), 175–186.

Lantos, G. (1970). "The flexural behavior of steel reinforced laminated timber beams." *Wood Sci.*, 2(3), 136–143.

Meier, U., Deuring, M., Meier, H., and Schwegler, G. (1992). "Strengthening of structures with CFRP laminates: research and applications in Switzerland." *Proc., 1st Int. Conf. on Advanced Composite Mat. in Bridges and Struct.*, Can. Soc. of Civ. Engrs., Sherbrooke, Canada, 243–251.

Mitzner, R. C. (1973). "Durability and maintenance of plywood overlaid with fiberglass reinforced plastic." *Am. Plywood Assoc. Res. Rep. No. 119, part 3*, American Plywood Association, Madison, Wisc.

Peterson, J. (1965). "Wood beams prestressed with bonded tension elements." *J. Struct. Engrg.*, ASCE, 91(1), 103–119.

Phillips, L. N., ed. (1979). *Design with advanced composite materials*. Springer-Verlag, London, England.

Plevris, N., and Triantafillou, T. (1992). "FRP-reinforced wood as structural material." *J. Mat. Civ. Engrg.*, ASCE, 4(3), 300–317.

Plevris, N., and Triantafillou, T. (1994). "Time-dependent behavior of RC members strengthened with FRP laminates." *J. Struct. Engrg.*, ASCE, 120(3), 1016–1042.

Preis, L., and Bell, T. A. (1986). "Fiberglass tendons for postensioning concrete bridges." *Transp. Res. Rec. 1118*, Nat. Res. Council, Washington, D.C., 77–82.

Saucier, J. R., and Holman, J. A. (1975). "Structural particleboard reinforced with glass fiber—progress in its development." *Forest Products J.*, 25(9), 69–72.
Sliker, A. (1962). "Reinforced wood laminated beams." *Forest Products J.* , 12(1), 91–96.
Stern, E. G., and Kumar, V. K. (1973). "Flitch beams." *Forest Products J.*, 23(5), 40–47.
Sturgeon, J. B. (1978). "Creep of fiber reinforced thermosetting resins." *Creep of engineering materials*, C. D. Pomeroy, ed., Mechanical Engineering Publications Limited, London, England.
Tang, R. C. (1980). "Viscoelastic behavior of wood in changing environments." *Proc., Workshop on How the Envir. Affects Lumber and Des. Assessments and Recommendations*, U.S. Dept. of Agric., Forestry Products Lab, Madison, Wisc., 115–121.
Taylor, R. J., Batchelor, B. deV., and Dalen, K. V. (1983). "Prestressed wood bridges." *Struct. Res. Rep. SRR-83-01*, Ministry of Transp. and Communication, Downsview, Ontario, Canada.
Theakston, F. H. (1965). "A feasibility study for strengthening timber beams with fiberglass." *Can. Agric. Engrg.*, (Jan.), 17–19.
Toratti, T. (1991). "Creep of wood in varying environment humidity; Part I: Simulation of creep." *Rep. 19*, Lab. of Struct. Engrg. and Bldg. Physics, Helsinki Univ. of Tech., Espoo, Finland.
Triantafillou, T. C., and Deskovic, N. (1992). "Prestressed FRP sheets as external reinforcement of wood members." *J. Struct. Engrg.*, ASCE, 118(5), 1270–1284.
van der Put, T. A. C. M. (1989a). *Deformation and damage processes in wood*. Delft Univ. Press, Delft, The Netherlands.
van der Put, T. A. C. M. (1989b). "Theoretical explanations of the mechano-sorptive effect in wood." *Wood Fiber Sci.*, 21(3), 219–230.

APPENDIX II. NOTATION

The following symbols are used in this paper:

A = axial rigidity;
$\tilde{A}$ = adjusted axial rigidity;
B = first moment of cross-sectional area;
$\tilde{B}$ = adjusted first moment of cross-sectional area;
B_ω = parameter associated with rate of change of wood-moisture factor;
b = width of cross section;
b_{fc} = width of fiber composite sheet;
D_1–D_{16} = creep model constants;
dt = time increment;
E_{eff} = effective modulus of wood;
E_v = viscoelastic modulus of fiber composite;
E_w = initial Young's modulus of wood;
E_0 = initial Young's modulus of fiber composite;
h = height of cross section;
I = moment of inertia with respect to top compressive fiber;
$\tilde{I}$ = adjusted moment of inertia with respect to top compressive fiber;
K_e = spring constant associated with elastic strain;
K_{e0} = spring constant associated with elastic strain at reference environment;
K_k = spring constant of Kelvin element;
K_{k0} = spring constant of Kelvin element at reference environment;
l = span length;
M = bending moment; actual moisture content;
M_0 = reference moisture content;
m = parameter in Findley's model;
N = axial force;
n = parameter in Findley's model;
T = actual temperature;
T_0 = reference temperature;
t = time; thickness of fiber composite sheet;
t_ω = time following a change in the environment humidity factor;
t_0 = parameter in Findley's model;
y = distance from top wood fiber;
α = fiber-reinforced plastic (FRP) creep coefficient;
β = wood creep coefficient;
ΔM = restraining moment;
ΔN = restraining axial force;
$\Delta\varepsilon_0$ = increment of strain at top wood fiber;
$\Delta\kappa$ = increment of curvature;
δ = midspan beam deflection;
ε = total strain;
ε_e = elastic strain;
ε_i = strain at distance y from top fiber;
ε_k = Kelvin strain;
ε_{ms} = mechanosorptive strain;
ε_v = viscoelastic strain;
ε_0 = initial FRP strain;

ε_{0i} = initial strain at top wood fiber;
θ = relative temperature factor;
κ = curvature;
κ_i = initial curvature;
μ_k = viscosity of Kelvin element;
μ_{k0} = viscosity of Kelvin element at reference environment;
μ_{ms} = viscosity of mechanosorptive element;
μ'_{ms} = mechanosorptive element constant with units of stress;
μ_v = viscosity associated with unrecoverable strain;
μ_{v0} = viscosity associated with unrecoverable strain at reference environment;
σ = stress;
σ_{fc} = stress in fiber composite;
σ_w = stress in wood;
σ_{wb} = wood bottom fiber stress;
σ_{wt} = wood top fiber stress;
ρ_{fc} = area fraction of fiber composite;
ω = wood-relative-moisture-content factor;
ω_e = environment-relative-moisture factor;
ω_f = final environment-relative-moisture factor; and
ω_i = initial environment-relative-moisture factor.